IU/NTC 97–09

The Nuclear Spin-Orbit Force in Chiral Effective Field Theories

R. J. Furnstahl and John J. Rusnak
Department of Physics
The Ohio State University, Columbus, OH 43210

Brian D. Serot
Department of Physics and Nuclear Theory Center
Indiana University, Bloomington, IN 47405

(September, 1997)

Abstract

A compelling feature of relativistic mean-field phenomenology has been the reproduction of spin-orbit splittings in finite nuclei after fitting only to equilibrium properties of infinite nuclear matter. This successful result occurs when the velocity dependence of the equivalent central potential that leads to saturation arises primarily because of a reduced nucleon effective mass. The spin-orbit interaction is then also specified when one works in a four-component Dirac framework. Here the nature of the spin-orbit force in more general chiral effective field theories of nuclei is examined, with an emphasis on the role of the tensor coupling of the isoscalar vector meson (ω) to the nucleon.

PACS number(s): 21.30.-x,12.39.Fe,12.38.Lg,24.85+p

I. INTRODUCTION

The concepts and methods of effective field theory (EFT) [1–5] have recently elucidated the successful nuclear phenomenology of relativistic field theories of hadrons, called quantum hadrodynamics (QHD) [6–9]. The EFT framework shows how QHD models can be consistent with the symmetries of quantum chromodynamics (QCD) and can be extended to accurately reproduce its low-energy features. The EFT perspective accounts for the success of relativistic mean-field models and provides an expansion scheme at the mean-field level and for going beyond it [8,10].

One of the most compelling features of QHD mean-field phenomenology is the reproduction of spin-orbit splittings in finite nuclei after fitting only to the equilibrium properties of infinite nuclear matter. This successful result occurs when the velocity dependence of the equivalent central potential that leads to saturation arises primarily because of a reduced nucleon effective mass. The spin-orbit interaction in nuclei is then also specified by the structure of the four-component Dirac spinors [9]. Does this connection survive in the extended EFT framework? Here we re-examine the nature of the spin-orbit force in chiral effective field theories of nuclei.

The strong correlation in QHD models between the effective mass M_0^* of the nucleon in equilibrium nuclear matter and the strength of the spin-orbit force in nuclei has been well documented [11–13,9]. Typical values of M_0^*/M in successful models are roughly 0.6, which yield spin-orbit splittings close to experimental values (e.g., 6 MeV for p states in ^{16}O). In Ref. [14], a wider class of models, which included variations of the linear sigma model as well as all of the standard QHD models used phenomenologically,[1] was studied systematically. Accurate reproductions of observables in finite nuclei, including the spin-orbit splitting in particular, tightly constrained the value of M_0^*/M to the range $0.58 \leq M_0^*/M \leq 0.64$.

In Ref. [8], an effective hadronic lagrangian consistent with the symmetries of QCD and intended for application to finite density systems was constructed. This involved a different strategy than in conventional QHD phenomenology. Rather than maximizing predictivity by minimizing the free parameters (as in renormalizable models), the goal was to test a systematic expansion for low-energy observables, which included the effects of hadron compositeness and the constraints of chiral symmetry. The degrees of freedom are (valence) nucleons, pions, and the low-lying non-Goldstone bosons. A scalar-isoscalar field with a mass of roughly 500 MeV was also included to simulate the exchange between nucleons of two correlated pions in this channel. The lagrangian was expanded in powers of the fields and their derivatives, with the terms organized using Georgi's "naive dimensional analysis" (NDA) [15,4,16]. The coefficient of each term is written as a combination of the pion-decay constant $f_\pi \approx 93$ MeV and a larger scale $0.5 \lesssim \Lambda \lesssim 1$ GeV times a dimensionless coupling constant. The effective lagrangian is said to be "natural" if these dimensionless coefficients are of order unity.

The result is a faithful representation of low-energy, non-strange QCD, as long as all

[1] These "conventional" QHD models typically include cubic and quartic self-couplings of the scalar field and sometimes a quartic self-coupling of the vector field, and they may also include one-loop vacuum corrections.

nonredundant terms consistent with symmetries are included. In addition, the mean-field framework provides a means of approximately including higher-order many-body and loop effects, since the scalar and vector meson fields play the role of auxiliary Kohn–Sham potentials in relativistic density functional theory [9]. Fits to nuclear properties at the mean-field level showed that the effective lagrangian could be truncated at the first few powers of the fields and their derivatives, with natural [$O(1)$] coefficients for each term. Of the two full parameter sets identified, one (model G2) provided an excellent fit, including spin-orbit splittings, with a nuclear matter value of $M_0^*/M \approx 0.66$. More recently, new parameters sets with excellent fits have been found with $M_0^*/M \approx 0.70$ [17].

An analogous study was made of relativistic "point-coupling" (PC) models in Ref. [10]. In these models, non-Goldstone mesons are not included explicitly. One instead has an expansion of the nucleon scalar and vector potentials in powers and derivatives of local nucleon scalar and vector densities. As in Ref. [8], an effective lagrangian consistent with chiral symmetry was constructed and fits to nuclear observables were made to test naturalness. Excellent fits were found with unprecedented values of M_0^*/M, as high as 0.74 at nuclear matter equilibrium.

Our purpose here is to examine the nature of the nuclear spin-orbit force in these generalized models. We find that the most important new feature affecting spin-orbit splittings in the lagrangians of Refs. [8] and [10] is the inclusion of a *tensor* coupling of the omega field to the nucleon (or its point-coupling analog). Because the effective lagrangian includes a derivative expansion, the tensor term appears at a relatively low order. None of the other new terms has a comparable impact on the spin-orbit strength.

We find a trade-off between the size of the scalar potential (or equivalently, the effective mass M^*) and the size of the tensor coupling. The existence of such a trade-off has been noted in previous studies of the isoscalar tensor coupling in QHD models, but good fits to nuclei were found only with relatively small values of the coupling and thus small $M_0^* \approx 0.6M$ [18,11]. Furthermore, this coupling is usually taken to be zero in one-boson-exchange potentials [19] or limited to small values due to constraints from *free* nucleon form factors and the assumption of vector meson dominance [20–23]. However, as an effective coupling in nuclei, which might absorb higher-order many-body effects at the mean-field level, the isoscalar tensor coupling could be much larger than these constraints dictate and still be of natural size.

In fits made using more complete meson and point-coupling models, larger (but still natural) values are favored, particularly in the point-coupling models [10]. In this work, we show that the increase in M_0^*/M in these models is well accounted for by the contribution from the tensor coupling. First, we consider two-component reductions of the models, which are reviewed in Sects. II and III. The spin-orbit potential in the two-component single-particle hamiltonian manifests the influence of both M_0^*/M and the tensor coupling, and a simple local-density approximation leads to quantitative predictions for the spin-orbit strength in nuclei. We find a strong correlation between the size of the isoscalar tensor coupling and the increase of M_0^*/M above 0.6. This discussion applies to a very general class of QHD models, including the quark-meson-coupling (QMC) model [24] and the Zimányi-Moszkowski (ZM) model [25] (both of which are found to be deficient).

A second approach is to transform the nucleon fields in models with tensor couplings. A feature of effective lagrangians is the freedom to perform field redefinitions without changing

the physics (if all nonredundant terms have been included). It is not possible to completely transform away the tensor interaction in a QHD effective lagrangian. To study the consequences for nucleon–nucleus scattering, however, we can perform an energy-dependent transformation to replace the potential in the Dirac equation with an equivalent potential (that is, one that generates the same scattering observables) with no tensor term [26]. The new scalar and vector potentials can then be compared to empirical optical potentials.

It is well known that in relativistic models applied to hypernuclei, the isoscalar tensor coupling of the omega to the hyperon plays a critical role in *reducing* the strength of the hyperon spin-orbit potential [27,28]. Quark-model arguments imply that the anomalous coupling is equal to (minus) the vector coupling, which leads to a strong cancellation between contributions to the spin-orbit force and therefore small splittings, as needed phenomenologically. To our knowledge, there is no corresponding implication for the tensor coupling of the omega to nucleons.[2]

II. SPIN-ORBIT FORCE AND M^* WITHOUT TENSOR COUPLING

In this section, we explore the relationship between the spin-orbit force and the nucleon potentials in models without tensor potentials. The connection between the spin-orbit splittings and the scalar and vector potentials is most easily seen by making a reduction to a two-component spin-orbit hamiltonian. We can write the isoscalar part of the Dirac single-particle hamiltonian (for spherical nuclei) as

$$h_0 = -i\boldsymbol{\nabla}\cdot\boldsymbol{\alpha} + \beta\Big(M - \Phi(r)\Big) + W(r) \ , \tag{1}$$

where M is the nucleon mass, Φ is the scalar potential, and W is the vector potential. A tensor potential is considered in the next section. Note that we need not assume that Φ is simply proportional to a scalar meson field ϕ. In fact, Φ could be proportional to ϕ (as in conventional QHD models), or could be expressed as a sum of scalar and vector densities (as in relativistic point-couplings models), or could be a nonlinear function of ϕ (as in the QMC and ZM models).

To leading-order in $1/M$, the spin-orbit term in a Foldy–Wouthuysen reduction of h_0 takes the form [6]

$$h_{\rm LS,FW} = \left[\frac{1}{4M^2 r}\left(\frac{d\Phi}{dr} + \frac{dW}{dr}\right) + O(1/M^3)\right]\boldsymbol{\sigma}\cdot\boldsymbol{L} \ \ . \tag{2}$$

The expansion is in powers of momenta (i.e., derivatives) and potentials divided by the nucleon mass.

The qualitative impact of the potentials on the spin-orbit force is clear from this expression and leads to some basic observations common to all successful models:

---

[2]We note, however, that in the SU(2) limit of a simple constituent quark model, in which the quarks have only Dirac magnetic moments and couple directly to the photon, the nucleon isoscalar magnetic moment is small [29].

1. Successful models are natural [8,10], which implies that the potentials closely follow the baryon density. This result follows from the equations for the potentials and the close relationship between scalar and vector densities,

$$\Phi(r) = \frac{\alpha_s}{f_\pi^2}\rho_{\rm s}(r) + O\left(\frac{\Phi^2}{M^2}, \frac{W^2}{M^2}, \frac{\nabla^2\Phi}{M^3}\right) \ , \tag{3}$$

$$W(r) = \frac{\alpha_v}{f_\pi^2}\rho_{\rm B}(r) + O\left(\frac{\Phi W}{M^2}, \frac{\nabla^2 W}{M^3}\right) \ , \tag{4}$$

where α_s and α_v are $O(1)$. The precise expressions for the constants α_s and α_v will depend on the model; for example, in conventional QHD models $\alpha_s = g_{\rm s}^2 f_\pi^2/m_{\rm s}^2$ and $\alpha_v = g_{\rm v}^2 f_\pi^2/m_{\rm v}^2$. In every case, however, naturalness implies that the corrections are order $\Phi/M \approx 1/3$ smaller than the leading term in the interior of nuclei and smaller still on the surface. Furthermore, the scalar density and baryon density are equal to within 5 to 10% at ordinary nuclear densities.

2. Thus a simple local density approximation for $\Phi(r)$ and $W(r)$ should be quite reasonable:

$$\Phi(r) \approx \Phi_0 \frac{\rho_{\rm B}(r)}{\rho_0} \ , \tag{5}$$

$$W(r) \approx W_0 \frac{\rho_{\rm B}(r)}{\rho_0} \ , \tag{6}$$

where Φ_0 and W_0 are the values of the potentials in nuclear matter at equilibrium density ρ_0. The remaining factor from the expectation value of $h_{\rm LS,FW}$ will be universal for different models, as long as they accurately reproduce nuclear density profiles.

3. The Hugenholtz–van Hove theorem relates Φ_0 and W_0 through the values of the chemical potential μ and the equilibrium Fermi momentum $k_{\rm F}$:

$$\mu = W_0 + \sqrt{k_{\rm F}^2 + M_0^{*2}} \ , \tag{7}$$

with $M_0^* \equiv M - \Phi_0$. Since μ and $k_{\rm F}$ are the same in all successful models to very good approximation [30,8], the dependence on W_0 can be eliminated in favor of Φ_0.

4. Therefore, the strength of the spin-orbit interaction (2) and the resulting magnitude of the splitting in nuclei should be, to a good approximation, directly proportional to the size of Φ_0, the scalar potential in nuclear matter.

If this analysis is quantitatively valid, we would expect to find that plots of spin-orbit splittings in nuclei versus equilibrium M_0^*/M for different models that reproduce nuclear density distributions would lie roughly on a straight line. Such plots are shown in Figs. 1–4 for splittings in ^{16}O, ^{40}Ca, and ^{208}Pb using a large number of models. The open circles are for QHD–I models [30,9] (the original linear Walecka model plus cubic and quartic scalar self-interactions). The circles marked with crosses also include one-loop vacuum corrections; this is essentially equivalent to adding a particular quintic scalar self-interaction term [31]. Each

QHD–I model was fit to a standard set of nuclear matter saturation conditions (equilibrium density, binding energy, and symmetry energy) and the charge radius of ^{40}Ca [30]. The diamonds are for QHD models from Ref. [8], squares are for point-coupling models from Refs. [32] and [10], and triangles are for QMC and ZM models from Refs. [24] and [33]. (The models with filled symbols contain tensor interactions and are discussed in Sect. III.) It is evident that there is a universal curve, but it is not a straight line except for M_0^* very close to M (i.e., small Φ), in contrast to the conclusion reached in point (4), above.

For a more *quantitative* local-density estimate of the spin-orbit splitting, we must go beyond leading order in the Foldy–Wouthuysen reduction, which is not an efficient expansion at finite density, even though $|\mathbf{p}|/M$ is quite small. The problem is that the Foldy–Wouthuysen expansion also involves Φ/M and W/M, which are less than unity but not negligible.

Reinhard has proposed a more useful expansion, which counts powers of a (relatively) small nucleon velocity v [11]. Specifically,

$$\begin{aligned}
\epsilon_\alpha/M \equiv (E_\alpha - M)/M \qquad &\longrightarrow \qquad \text{order } v^2 \ , \\
(\Phi - W)/M \qquad &\longrightarrow \qquad \text{order } v^2 \ , \\
M^*/M = (M - \Phi)/M \qquad &\longrightarrow \qquad \text{order } 1 \ , \\
\frac{\boldsymbol{\sigma}\cdot\boldsymbol{p}}{M}\,\frac{M}{M + E_\alpha - \Phi - W}\,\frac{\boldsymbol{\sigma}\cdot\boldsymbol{p}}{M} \qquad &\longrightarrow \qquad \text{order } v^2 \ .
\end{aligned} \tag{8}$$

Here E_α is the energy eigenvalue for state α, including the rest mass. Since nuclei are weakly bound, the kinetic energy proportional to v^2 balances the net potential energy $\approx \Phi - W$, which leads to the first two results. But while the difference of the potentials is counted as a small quantity, the potentials themselves are not. On the other hand, they are still small enough compared to M to count M^*/M as order 1, which explains the final two counting rules.

Reinhard's procedure constructs order-by-order in v^2 a single-particle hamiltonian $h_{\rm NR}$ that acts on two-component (normalized) wavefunctions [11]. The latter are related to the upper components of the Dirac four-component wavefunctions by a normalization operator. He equates the expectation value $\langle h_0 - E_\alpha\rangle$ calculated with the four-component wavefunctions with the corresponding expectation value $\langle h_{\rm NR} - \epsilon_\alpha\rangle$ calculated with the two-component wavefunctions. This condition specifies $h_{\rm NR}$ at each order in v^2, up to corrections of the next order.

We have considered two possibilities for the spin-orbit part of $h_{\rm NR}$ to order v^2,

$$h_{\rm LS,R} = \Big[\frac{1}{2r}\frac{d}{dr}\frac{1}{\overline{M}(r)} + O(v^4)\Big]\boldsymbol{\sigma}\cdot\boldsymbol{L} = \Big[\frac{1}{4\overline{M}^2}\frac{1}{r}\left(\frac{d\Phi}{dr} + \frac{dW}{dr}\right) + O(v^4)\Big]\boldsymbol{\sigma}\cdot\boldsymbol{L} \ . \tag{9}$$

where $\overline{M}(r)$ is defined as

$$\overline{M}(r) \equiv M - \frac{1}{2}\Big(\Phi(r) + W(r)\Big) \ , \tag{10}$$

and

$$h'_{\rm LS,R} = \Big[\frac{1}{2r}\frac{d}{dr}\frac{1}{M^*(r)} + O(v^4)\Big]\boldsymbol{\sigma}\cdot\boldsymbol{L} = \Big[\frac{1}{2M^{*2}}\frac{1}{r}\frac{d\Phi}{dr} + O(v^4)\Big]\boldsymbol{\sigma}\cdot\boldsymbol{L} \ . \tag{11}$$

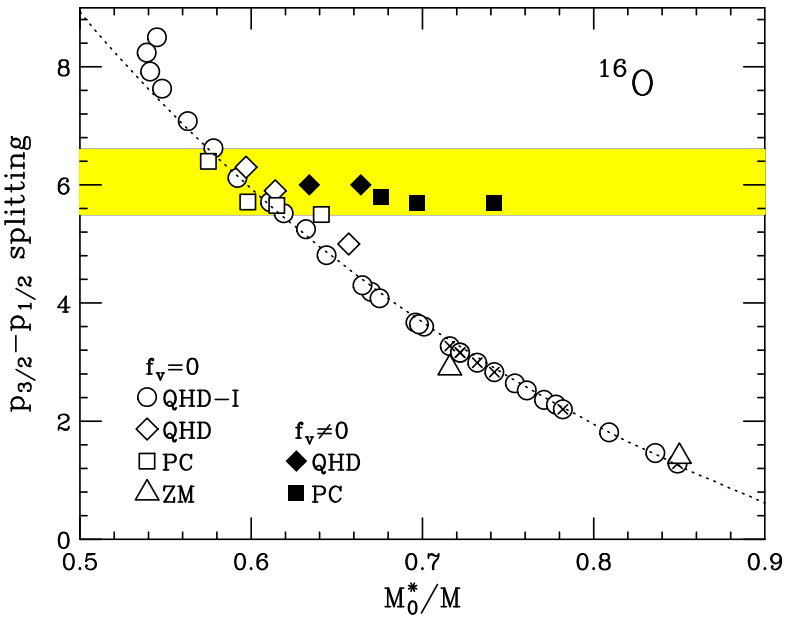

FIG. 1. Spin-orbit splitting for the proton p states in ^{16}O vs. equilibrium M_0^*/M for a variety of models. The shaded band is an estimate of the experimental uncertainty. Open symbols are for models with tensor coupling $f_{\rm v} = 0$ and filled symbols are for models with $f_{\rm v} \neq 0$. The dotted curve follows from Eq. (14). See the text for descriptions of the models.

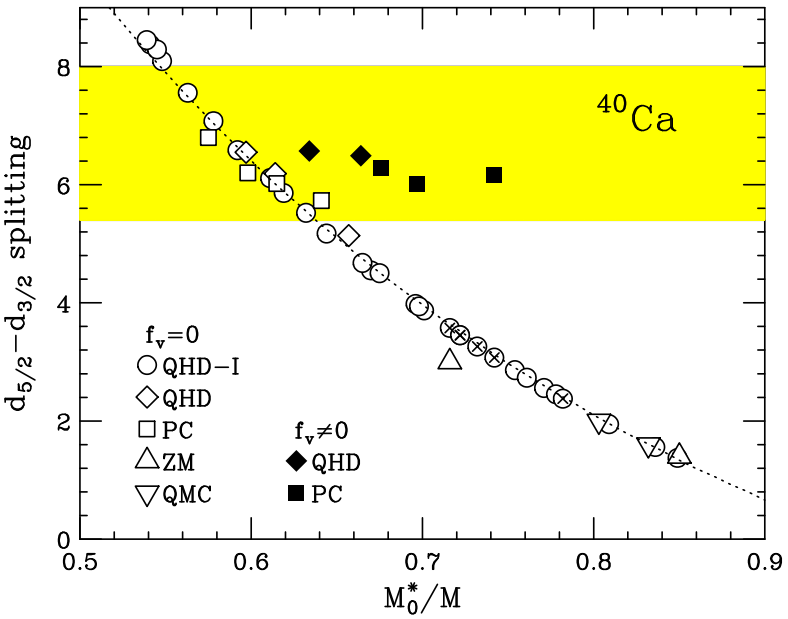

FIG. 2. Same as Fig. 1 for the proton d states in ^{40}Ca.

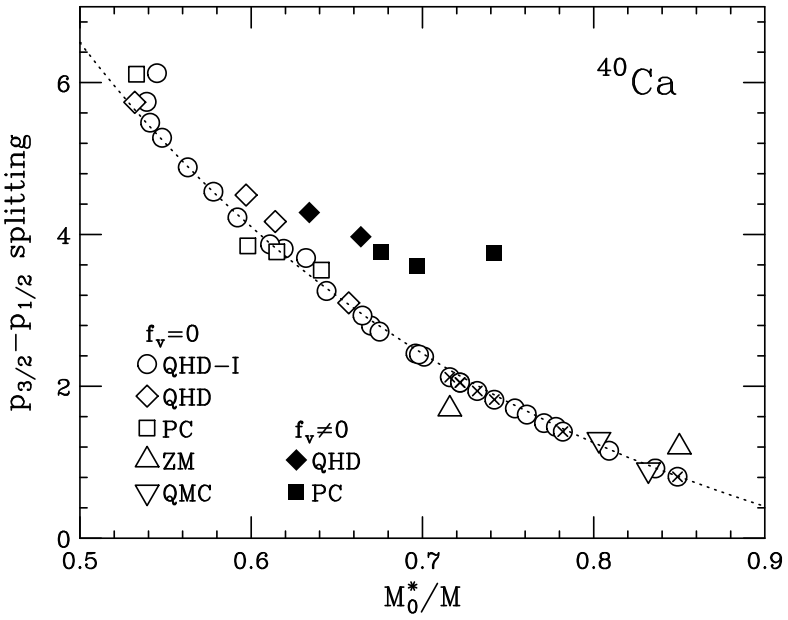

FIG. 3. Same as Fig. 1 for the proton p states in ^{40}Ca.

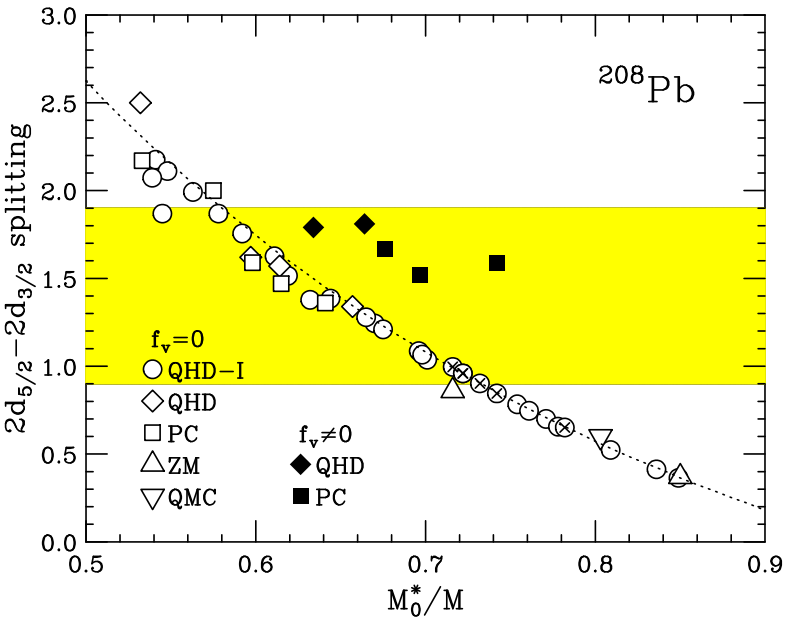

FIG. 4. Same as Fig. 1 for the proton $2d$ states in ^{208}Pb.

We have also constructed the $O(v^4)$ corrections to each. By taking explicit matrix elements of $h_{\rm LS,R}$ and $h'_{\rm LS,R}$ using two-component wavefunctions for spin-orbit pairs and comparing to the energy eigenvalues for the corresponding Dirac wavefunctions, we can determine the accuracy of these truncations. We find that $h_{\rm LS,R}$ systematically underpredicts the splittings by roughly 5% while $h'_{\rm LS,R}$ overpredicts the splittings by about 15%. The predictions using the $O(v^4)$ hamiltonians are quite similar in the two cases and are within 3% of the Dirac splittings. We will use $h_{\rm LS,R}$ to $O(v^2)$ in the sequel.

We can estimate spin-orbit splittings as follows. We use the local-density expressions from Eqs. (5) and (6) in the numerator of Eq. (9) and replace $\overline{M}$ in the denominator by an average value

$$\langle\overline{M}\rangle = \frac{1}{2}(M + \langle M^*\rangle - \langle W\rangle) \ . \tag{12}$$

We use an interpolated value of M^*:

$$\langle M^*\rangle \equiv M_0^* + y(M - M_0^*) \ , \tag{13}$$

and Eq. (7) to define $\langle W\rangle$ given $\langle M^*\rangle$. One would expect y to be given roughly by $y \approx 1 - \langle\rho\rangle/\rho_0$, where $\langle\rho\rangle$ is an average density seen by the nucleons making up the spin-orbit pair. In ^{40}Ca, this would imply $y \approx 0.2$ for the p states and $y \approx 0.4$ for the d states. So the energy splitting takes the form

$$\epsilon_{\rm splitting} = C\,\frac{M - \overline{M}_0}{\langle\overline{M}\rangle^2}\,\delta\langle\boldsymbol{\sigma}\cdot\boldsymbol{L}\rangle \ , \tag{14}$$

where the constant C depends on the average of $(1/r)d\rho_{\rm B}/dr$ over the nucleus (which is essentially the same for the members of a spin-orbit pair), and $\delta\langle\boldsymbol{\sigma}\cdot\boldsymbol{L}\rangle$ is the difference in the expectation values of $\boldsymbol{\sigma}\cdot\boldsymbol{L}$ for the spin-orbit pair. The nuclear matter value $\overline{M}_0$ follows from M_0^*/M using Eqs. (10) and (7).

This local-density estimate of the splitting as a function of nuclear matter M_0^*/M is shown in Figs. 1–4 as a dotted line. The curves are normalized to the point with the largest value of M_0^*/M to absorb the constant C and any overall normalization errors. The least-bound states are well fit with $y = 0.4$, and the deeply bound states, with $y = 0.2$. The local-density estimates account quantitatively for the spin-orbit trend.[3]

The shaded regions in Figs. 1, 2, and 4 indicate the empirical spin-orbit splittings. Since we do not calculate rearrangement effects, there are intrinsic uncertainties in comparing to experimental splittings.[4] We have therefore been conservative in defining these regions.

---

[3]Note that fitting to a different charge radius for ^{40}Ca shifts the dotted curve up (for a smaller radius) or down (for a larger radius). That is why the open diamonds tend to be slightly above the curve, since the ^{40}Ca radius used is 3.45 fm rather than 3.48 fm as in the other models.

[4]In addition, the Kohn–Sham nature of our calculation implies that the single-particle energy eigenvalues do not correspond precisely to observables [9]. Nevertheless, we expect that *differences* in eigenvalues are good estimates of the splitting, at least near the Fermi surface.

However, the intersection of the universal curve with each region implies that models with effective masses outside the range $0.58 \leq M_0^*/M \leq 0.64$ proposed in Ref. [14] will not be able to reproduce empirical spin-orbit splittings (when there is no tensor coupling). This is true of the QMC [24] and ZM [25] models, which are indicated by triangles in Figs. 1–4.

One of the appealing features of relativistic models is that one can come to a similar conclusion about M_0^*/M without considering spin-orbit splittings. For example, the study by Rufa et al. [18] of conventional QHD–I models (i.e., the linear Walecka model plus cubic and quartic scalar meson self-couplings) revealed that a good fit to bulk nuclear properties *excluding spin-orbit splittings* still required M_0^*/M to be close to 0.6 at equilibrium.

This result can be understood in terms of a key feature of relativistic models: the additional saturation mechanism that arises from a Lorentz scalar interaction. The velocity dependence in the interaction due to the scalar potential appears in the energy of nuclear matter (to leading order in k^2) as a modification of the kinetic energy per particle:

$$\left\langle \frac{k^2}{2M} \right\rangle \longrightarrow \left\langle \frac{k^2}{2M^*} \right\rangle = \frac{3}{5}\frac{k_{\rm F}^2}{2M}\left(\frac{M}{M^*(\rho_{\rm B})}\right) \ . \tag{15}$$

The extra density-dependent repulsion from the M/M^* factor leads to saturation [9]; in successful mean-field models (which include QHD–I models with $0.58 \leq M_0^*/M \leq 0.64$) it is the dominant saturation mechanism. In these cases, a fit to the nuclear matter equilibrium density and binding energy alone constrains M_0^*/M and the implied velocity dependence; the four-component structure of the Dirac wave functions then *automatically* generates an appropriate spin-orbit force in finite nuclei. In contrast, in QHD–I models with larger values of M_0^*/M, the empirical equilibrium point is obtained from repulsive three- and four-body contributions that become more and more important as M_0^*/M increases.

In summary, models without isoscalar tensor couplings exhibit a strong correlation between the effective nucleon mass at nuclear matter equilibrium density and the spin-orbit splittings in nuclei. Comparison to experiment reinforces the constraint $0.58 \leq M_0^*/M \leq 0.64$ for successful models of this type. Next we consider the generalization that includes tensor couplings.

III. TENSOR COUPLING AND SPIN-ORBIT SPLITTING

We generalize h_0 from Eq. (1) by adding a tensor potential $T(r)$:

$$h_1 = -i\boldsymbol{\nabla}\cdot\boldsymbol{\alpha} + \beta\Big(M - \Phi(r)\Big) + W(r) - i\beta\boldsymbol{\alpha}\cdot\widehat{\boldsymbol{r}}\,T(r) \ . \tag{16}$$

A tensor potential of this form arises in a meson model from the tensor coupling of an isoscalar vector meson (ω) to the nucleon. Using the conventions of Ref. [8],

$$\mathcal{L}_{\rm tensor} = -\frac{f_{\rm v} g_{\rm v}}{4M}\overline{N}\sigma^{\mu\nu}N\left(\partial_\mu V_\nu - \partial_\nu V_\mu\right) \ , \tag{17}$$

which implies

$$T(r) = \frac{f_{\rm v}}{2M}\frac{dW}{dr} \ . \tag{18}$$

(Note that $f_{\rm v}$ as defined here corresponds to the combination $f_{\rm v}/g_{\rm v}$ typically appearing in one-boson-exchange models [19].) The analog of Eq. (17) in the point-coupling model of Ref. [10] is

$$\mathcal{L}_{\rm tensor} = -\frac{\widetilde{f}_{\rm v}}{f_\pi^2 \Lambda} \overline{N} \sigma^{\mu\nu} N \, \partial_\mu (\overline{N} \gamma_\nu N) \ , \tag{19}$$

which implies

$$T(r) = \frac{\widetilde{f}_{\rm v}}{f_\pi^2 \Lambda} \frac{d\rho_{\rm B}}{dr} \ . \tag{20}$$

Thus we can make the rough correspondence $f_{\rm v} \leftrightarrow 2\widetilde{f}_{\rm v}$. [Note that a spin-2 meson in the (1,1) representation is described by a *symmetric* tensor $f^{\mu\nu}$. Thus it does not couple to $\overline{N}\sigma^{\mu\nu}N$ and will not produce a tensor potential at the mean-field level.]

We repeat the procedure that led to Eq. (9) to find

$$h_{\rm LS,T} = \left[\frac{1}{4\overline{M}^2} \frac{1}{r} \left(\frac{d\Phi}{dr} + \frac{dW}{dr} \right) + \frac{f_{\rm v}}{2M\overline{M}} \frac{1}{r} \frac{dW}{dr} + O(v^4) \right] \boldsymbol{\sigma} \cdot \boldsymbol{L} \ , \tag{21}$$

and the result for point-coupling models is found from the substitution

$$\frac{f_{\rm v}}{M} \frac{dW}{dr} \longrightarrow \frac{2\widetilde{f}_{\rm v}}{\Lambda f_\pi^2} \frac{d\rho_{\rm B}}{dr} \ . \tag{22}$$

Now suppose that we want to know how M^* in a model with $f_{\rm v} \neq 0$ compares to the value $M^*_{f_{\rm v}=0}$ in an "equivalent" model with $f_{\rm v} = 0$. If we define "equivalent" to mean that they have the same spin-orbit strength, we can use Eq. (21) to make a rough comparison. Let us assume the local-density relations from Eqs. (5) and (6), so that if we equate $h_{\rm LS,T}$ in the two models, the r dependence cancels (in an averaged sense), and we have the condition

$$\left. \frac{M - \langle \overline{M} \rangle}{\langle \overline{M} \rangle^2} \right|_{f_{\rm v}=0} = \frac{M - \langle \overline{M} \rangle}{\langle \overline{M} \rangle^2} + \frac{f_{\rm v} \langle W \rangle}{M \langle \overline{M} \rangle} \ . \tag{23}$$

The analogous condition for the point-coupling models follows after applying Eq. (22).

We can use Eqs. (23) and (7) to transform the region $0.58 \lesssim (M_0^*/M)_{f_{\rm v}=0} \lesssim 0.64$, which applies to $f_{\rm v} = 0$, to the "equivalent" region for $f_{\rm v} > 0$ or $\widetilde{f}_{\rm v} > 0$. Values of $\langle \overline{M} \rangle$ and $\langle \overline{M} \rangle_{f_{\rm v}=0}$ are defined by Eq. (12) in terms of M_0^* and $(M_0^*)_{f_{\rm v}=0}$ using Eq. (13) with $y = 0.2$, and then $\langle W \rangle$ and $\langle W \rangle_{f_{\rm v}=0}$ follow from Eq. (7). One then inverts the resulting relation for M_0^* given an input $(M_0^*)_{f_{\rm v}=0}$.

The transformed regions are shown in Figs. 5 and 6, along with diamonds and squares marking the generalized ($f_{\rm v} \neq 0$) models from Refs. [8], [10] and [17]. While the shaded regions are not definitive indicators of the relation between the tensor coupling and M^* in successful models, they should provide a reliable estimate of the basic trend. Evidently, the bands are consistent with the models with nonzero tensor coupling that were fit directly to nuclei. These results are also consistent with new fits in the point-coupling models from Ref. [10], in which $\widetilde{f}_{\rm v}$ is held fixed at zero. The new sets have $(M_0^*/M)_{f_{\rm v}=0}$ between 0.60 and 0.64.

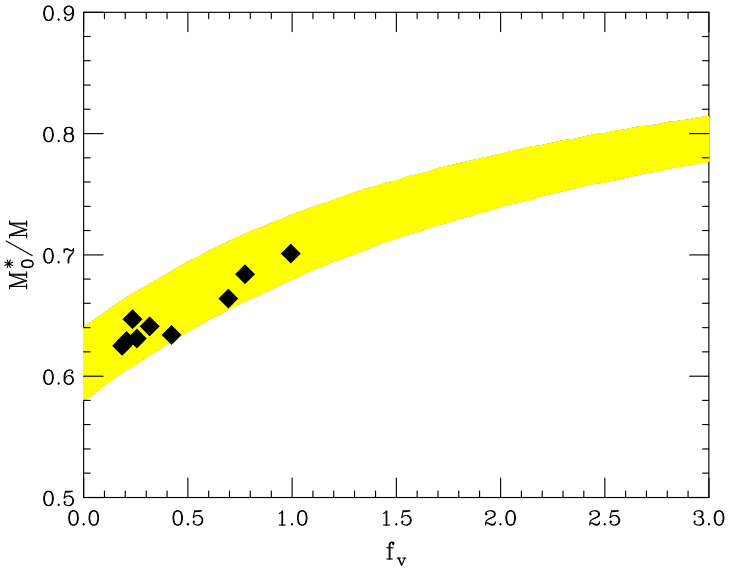

FIG. 5. Correlation between the isoscalar tensor coupling $f_{\rm v}$ and the effective mass in successful mean-field models with mesonic degrees of freedom. The shaded region shows the range M_0^*/M for a given value of $f_{\rm v}$ that corresponds to the range $0.58 \leq M_0^*/M \leq 0.64$ with $f_{\rm v} = 0$, found using Eq. (23). The QHD models, shown as filled diamonds, are direct fits to nuclear observables from Refs. [8] and [17].

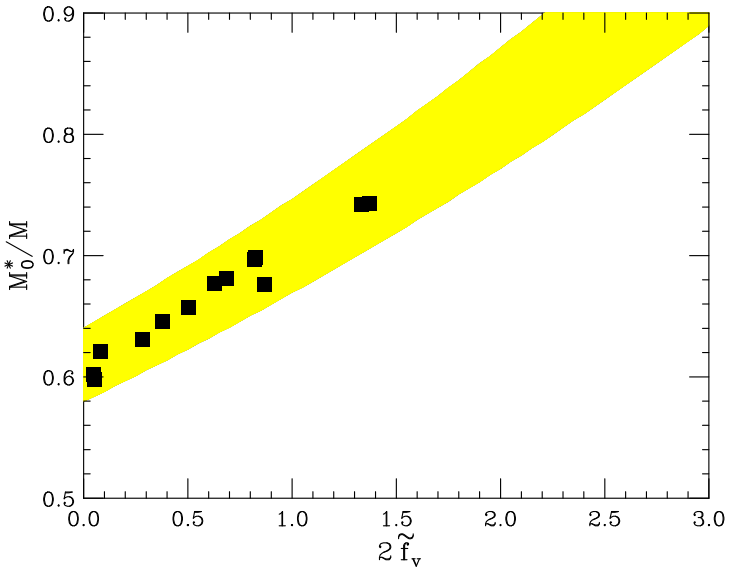

FIG. 6. Correlation between the isoscalar tensor coupling $\widetilde{f}_{\rm v}$ and the effective mass in successful mean-field point-coupling models. The shaded region shows the range M_0^*/M for a given value of $\widetilde{f}_{\rm v}$ that corresponds to the range $0.58 \leq M_0^*/M \leq 0.64$ with $\widetilde{f}_{\rm v} = 0$, found using Eq. (23). The point-coupling models, shown as filled squares, are direct fits to nuclear observables from Ref. [10].

As part of an extensive optimization analysis of conventional QHD models, Rufa et al. considered including an isoscalar tensor coupling [18]. They noted the trade-off between the magnitude of the spin-orbit splitting and the size of the scalar field. However, their chi-squared optimization yielded only a small improvement from the new term,[5] and the best value had a small value of $f_\mathrm{v} \approx 0.3$. (Note that their conventions differ from ours by a minus sign.) Reinhard concludes that including the tensor would make a difference only in the details, but not in the qualitative picture [11].

In Ref. [25], Biró and Zimányi propose adding a tensor coupling of the ω meson to the nucleon to the lagrangian proposed by Zimányi and Moszkowski [34], in order to bring the spin-orbit force up to the strength implied by nuclear spin-orbit splittings. They perform a similar expansion to the one above. However, the value of M_0^*/M in the ZM model is roughly 0.85. Figure 5 shows that this would require a very large value of f_v, which does not appear to be compatible with good fits to nuclear observables.

What constraints exist on the value of f_v? In free space there are constraints from nucleon electromagnetic form factors under the assumption of vector dominance. Depending on the form of vector dominance (i.e., tensor or vector representation [35]), we obtain a limit on f_v from the isoscalar anomalous moment of the nucleon or from the isoscalar magnetic radius of the nucleon. In either case, one finds the small value $|f_\mathrm{v}| \lesssim 0.2$ [20–23]. From Fig. 5, we see that such a limit implies an unimportant change in M^* from the results with $f_\mathrm{v} = 0$. In one-boson-exchange potentials, the *isovector* tensor coupling is important, but the isoscalar tensor coupling is usually taken to be zero [19]. On the other hand, without further assumptions, the value of $\widetilde{f}_\mathrm{v}$ in the point-coupling models is not related to the electromagnetic structure of the nucleon and is therefore unconstrained.

It is important to remember, however, that the mean-field parameters obtained from fitting to finite nuclei can be very different from the "free-space" tree-level values. These mean-field parameters must incorporate the effects of many-body physics beyond the Hartree level, which could induce strong renormalizations. We anticipate that isovector couplings will be less affected (since the free-space values are already of natural size and nuclei have roughly equal numbers of neutrons and protons), and therefore argue that fitting isovector parameters using free-space electromagnetic form factors is a good approximation. However, the situation with isoscalar parameters is unclear. We might even expect that in the absence of symmetry constraints in the medium, they take natural values. This would mean that any values shown in Figs. 5 or 6 are accessible (here, as in Ref. [8], $f_\mathrm{v}/4$ is the natural combination).

One might hope to constrain the value of f_v from the energy dependence of the optical potential. A single-particle hamiltonian of the form h_0 in Eq. (1) implies an energy-dependent optical potential for nucleon-nucleus scattering of the form [6]

$$V_\mathrm{opt}(r;\Phi,W) = 2EW(r) - W(r)^2 + M^*(r)^2 - M^2 \ . \tag{24}$$

If the potential $V_\mathrm{opt}(r)$ follows the nuclear density, the slope in energy is given by $2W_0$ [see

[5]The larger values of f_v and $\widetilde{f}_\mathrm{v}$ from optimized fits in Refs. [8,17,10] also yielded only a small improvement in χ^2 (a reduction of about one out of forty) compared to similar models with these parameters fixed at zero.

Eq. (6)], and is constrained by low-energy neutron-nucleus scattering to be about $0.6\,M$ [36,6]. To be consistent with experiment, W_0 must be as large as the values implied by $0.58 \leq M_0^*/M \leq 0.64$ through Eq. (7). The larger values of M_0^*, and consequently smaller values of W_0, when $f_\mathrm{v} > 0$ (or $\widetilde{f}_\mathrm{v} > 0$) could set a limit on the magnitude of the tensor coupling.

We cannot identify V_opt directly from h_1 because of the tensor potential. However, we can apply field redefinitions to the nucleon wavefunctions, so that the transformed version of Eq. (16) does not contain a tensor potential. Such a transformation was applied to Dirac wavefunctions in Ref. [26]. Given a solution $\psi(\mathbf{r})$ that satisfies $h_1\psi(\mathbf{r}) = E\psi(\mathbf{r})$ for scattering states ($E > M$), we define a transformed wavefunction $\phi(\mathbf{r})$ by

$$\phi(\mathbf{r}) = e^{-U(r)\gamma_0}\psi(\mathbf{r}) \ , \tag{25}$$

where $U(r) = f_\mathrm{v}W(r)/2M$ in the meson model and $U(r) = \widetilde{f}_\mathrm{v}\rho_\mathrm{B}(r)/f_\pi^2\Lambda$ in the point-coupling model. The function $U(r)$ goes to zero rapidly outside the nucleus, so scattering observables are unchanged.

The new wavefunction ϕ satisfies

$$\Big[-i\boldsymbol{\alpha}\cdot\boldsymbol{\nabla} + We^{2U\gamma_0} + \beta(M-\Phi)e^{2U\gamma_0}\Big]\phi_\alpha(\mathbf{r}) = Ee^{2U\gamma_0}\phi(\mathbf{r}) \ . \tag{26}$$

By rewriting the exponents we can make the identifications:

$$M^*_{f_\mathrm{v}=0} = M^*\cosh 2U + (W-E)\sinh 2U \ , \tag{27}$$

$$W_{f_\mathrm{v}=0} = E \ + (W-E)\cosh 2U + M^*\sinh 2U \ . \tag{28}$$

Therefore the transformation introduces energy dependence into the effective scalar and vector potentials. If evaluated in nuclear matter for $E \approx \mu$, the *predicted* values of $(M_0^*)_{\widetilde{f}_\mathrm{v}=0}$ and $(W_0)_{\widetilde{f}_\mathrm{v}=0}$ for the point-coupling models with $\widetilde{f}_\mathrm{v} \neq 0$ are consistent with Fig. 6; in particular, one obtains $0.58 \leq (M_0^*/M)_{\widetilde{f}_\mathrm{v}=0} \leq 0.61$ for each model shown. The predicted values for the QHD models in Fig. 5, however, are slightly smaller than expected [$(M_0^*/M)_{f_\mathrm{v}=0}$ is roughly 0.55].

If we use $M^*_{f_\mathrm{v}=0}$ and $W_{f_\mathrm{v}=0}$ from Eqs. (27) and (28) to evaluate the optical potential in Eq. (24), we find

$$V_\mathrm{opt}(r;\Phi_{f_\mathrm{v}=0}, W_{f_\mathrm{v}=0}) = V_\mathrm{opt}(r;\Phi,W) \ . \tag{29}$$

That is, the additional energy dependence in Eqs. (27) and (28) cancels out when evaluating V_opt. Thus the energy dependence of the optical potential is simply proportional to the *untransformed* vector potential W and is *independent* of f_v (or $\widetilde{f}_\mathrm{v}$). If the tensor coupling is too large, Figures 5 and 6 imply that W_0 will be too small to account for the experimental energy dependence. Therefore, smaller values of f_v (or $\widetilde{f}_\mathrm{v}$) are favored, with an upper limit around unity. This analysis is not conclusive, however, since the radial dependence of the potentials may invalidate the simple argument leading to the comparison with experiment [6]. This issue will be considered in future work.

IV. SUMMARY

We examined the role of an isoscalar tensor coupling to the nucleon in chiral effective lagrangians for nuclei. Effective lagrangians must contain all nonredundant terms consistent with the underlying symmetries. Since tensor couplings of the vector mesons to the nucleon (or their analogs in point-coupling models) will appear at low order in an expansion in powers of fields (or densities) and derivatives, they should be included.

In models that ignore such couplings, there is a strong correlation between the value of the nucleon effective mass M_0^* at equilibrium nuclear matter density and spin-orbit splittings in nuclei. In fact, given a value of M_0^*, one can predict the *calculated* splittings of weakly bound levels to an accuracy of roughly 0.3 MeV. Moreover, to accurately reproduce the *empirical* splittings, one requires an equilibrium M_0^*/M between 0.58 and 0.64. Interestingly, similar values of M_0^* are obtained when fits are performed without including information from these splittings.

When an isoscalar tensor coupling is included and allowed to vary freely, fits to nuclear properties slightly favor natural-sized values of the coupling, which are significantly larger than values deduced from free-space electromagnetic observables. This is particularly true in point-coupling models. These larger values of the coupling modify the simple relationship between M_0^* and the spin-orbit splittings noted above; however, it is possible to estimate the contribution of the tensor interaction to the spin-orbit force and to show that the larger values of M_0^* obtained in nuclear matter are consistent with the observed splittings.

We emphasize that the small size of the isoscalar tensor coupling deduced from free-space electromagnetic data is not incompatible with the larger values obtained in fits to nuclei, since the in-medium parameters must contain many-body effects. In all of the models discussed here, the resulting tensor coupling is still natural. It remains to be seen whether explicit calculation of the many-body contributions can account for the larger values favored by nuclei. Moreover, it may be possible to constrain the tensor coupling by including additional observables in the fits; the energy dependence of the optical potential for nucleon-nucleus scattering is a promising candidate.

ACKNOWLEDGMENTS

We thank B. C. Clark for useful discussions. This work was supported in part by the Department of Energy under Contracts No. DE–FG02–87ER40365 and DE–FG02–87ER40328, and the National Science Foundation under Grants No. PHY–9511923 and PHY–9258270. We thank the Department of Energy's Institute for Nuclear Theory at the University of Washington for its hospitality and the Department of Energy for partial support during the completion of this work.

REFERENCES

[1] S. Weinberg, Physica **A96** (1979) 327.

[2] G. P. Lepage, in *From Actions to Answers* (TASI-89), edited by T. DeGrand and D. Toussaint (World Scientific, Singapore, 1989), p. 483.

[3] J. Polchinski, in *Recent Directions in Particle Theory: From Superstrings and Black Holes to the Standard Model* (TASI-92), edited by J. Harvey and J. Polchinski (World Scientific, Singapore, 1993), p.235.

[4] H. Georgi, Ann. Rev. Nuc. Part. Sci. **43** (1993) 209.

[5] S. Weinberg, *The Quantum Theory of Fields, vol. I: Foundations* (Cambridge University Press, New York, 1995).

[6] B. D. Serot and J. D. Walecka, Adv. Nucl. Phys. **16** (1986) 1.

[7] B. D. Serot, Rep. Prog. Phys. **55** (1992) 1855.

[8] R. J. Furnstahl, B. D. Serot, and H.-B. Tang, Nucl. Phys. **A615** (1997) 441.

[9] B. D. Serot and J. D. Walecka, Int. J. Mod. Phys. E (1997), in press.

[10] John J. Rusnak and R. J. Furnstahl, Ohio State preprint, nucl-th/9708040, (1997).

[11] P.-G. Reinhard, Rep. Prog. Phys. **52** (1989) 439.

[12] Y. K. Gambhir, P. Ring, and A. Thimet, Ann. of Phys. **198** (1990) 132.

[13] A. R. Bodmer, Nucl. Phys. **A526** (1991) 703.

[14] R. J. Furnstahl, H.-B. Tang, and B. D. Serot, Phys. Rev. C **52** (1995) 1368.

[15] H. Georgi and A. Manohar, Nucl. Phys. **B234** (1984) 189.

[16] J. L. Friar, D. G. Madland, and B. W. Lynn, Phys. Rev. C **53** (1996) 3085.

[17] John J. Rusnak, Ph.D thesis, Ohio State University, 1997.

[18] M. Rufa, P.-G. Reinhard, J. A. Maruhn, W. Greiner, and M. R. Strayer, Phys. Rev. **C38** (1988) 390.

[19] R. Machleidt, Adv. Nucl. Phys. **19** (1989) 189.

[20] G. Höhler, E. Pietarinen, I. Sabba-Stefanescu, F. Borkowski, G. G. Simon, V. H. Walther, and R. D. Wendling, Nucl. Phys. **B114** (1976) 505.

[21] G. E. Brown, M. Rho, and W. Weise, Nucl. Phys. **A454** (1986) 669.

[22] Ulf-G. Meissner, Phys. Rep. **161** (1988) 213.

[23] P. Mergell, Ulf-G. Meissner, and D. Drechsel, Nucl. Phys. **A596** (1996) 367.

[24] K. Saito, K. Tsushima, A. W. Thomas, Nucl. Phys. **A609** (1996) 339.

[25] T. S. Biró and J. Zimányi, Phys. Lett. B **391** (1997) 1.

[26] B. C. Clark, S. Hama, and S. G. Kälbermann, E. D. Cooper, and R. L. Mercer, Phys. Rev. C **31** (1985) 694.

[27] B. Jennings, Phys. Lett. B **246** (1990) 325; Nucl. Phys. **A529** (1991) 589.

[28] J. Cohen and H. J. Weber, Phys. Rev. C **44** (1991) 1181.

[29] J. F. Donoghue, E. Golowich, and B. R. Holstein, *Dynamics of the Standard Model* (Cambridge University Press, New York, 1992).

[30] R. J. Furnstahl, C. E. Price, and G. E. Walker, Phys. Rev. C **36** (1987) 2590.

[31] R. J. Furnstahl, B. D. Serot, and H.-B. Tang, Nucl. Phys. **A618** (1997) 446.

[32] B. A. Nikolaus, T. Hoch, D. G. Madland, Phys. Rev. C **46** (1992) 1757.

[33] M. Chiapparini, A. Delfino, M. Malheiro, A. Gattone, Z. Phys. A **357** (1997) 47.

[34] J. Zimányi and S. Moszkowski, Phys. Rev. C **42** (1990) 1416.

[35] B. Borasoy and Ulf-G. Meissner, Int. J. Mod. Phys. **A111** (1996) 5183.

[36] P. J. Siemens and A. S. Jensen, *Elements of Nuclei* (Addison-Wesley, 19987).